07;08

Electron-photon interactions in the conditions of dimensional conductivity restrictions in semiconductor single quantum-size particles in interelectrodic nanogap

© N.D. Zhukov[1], M.V. Gavrikov[1,2], A.G. Rokakh[2]

[1] OOO NPP „Volga“, Saratov, Russia
[2] Saratov National Research State University, Saratov, Russia
E-mail: ndzhukov@rambler.ru

Received October 13, 2022
Revised December 7, 2022
Accepted December 8, 2022

For quantum-size particles of the InSb, PbS, HgSe, CdSe semiconductors, a model of competition of dimensional quantum restrictions and blocking with a single-electron current and Coulomb restriction, as well as heating electrons with an electric field of the light wave, is proposed. This made it possible to explain the highly multiplicity (up to two orders of order) of a change in photoconductivity observed in conditions of tunnel conductivity, and in the conditions of the confinement — the absence of inter-zone and inter-level photoconductivity. The resonant current peaks of quantum conductivity observed on the V-I characteristics when irritating with light of any wavelength (in the interval of $0.4-1.2\,\mu$m) are reset or shifted towards smaller voltage values. The energy minimum of quanta recorded in this case is estimated as 100 meV. The results can be useful in resolving issues of application in uncooled IR detectors, including single-photon registration.

Keywords: Quantum-size particle, dimensional quantification, one-electron current, single-photon process, inter-zone and intra-zone transitions, tunnel conductivity, Coulomb restriction, quantum conductivity.

DOI: 10.21883/TPL.2023.02.55367.19393

The examination of electron–photon interactions in the conditions of electron conductivity in quantum dots and quantum-dimensional particles (QPs) is of great applied and academic importance in the context of potential fabrication of nanocells, which are to be used as base elements of nanoelectronics and nanophotonics [1–3]. In addition to generation-recombination interband processes, which govern luminescence, optical absorption, and photoconductivity, they may feature intraband variations of electron states and single-electron transport with the manifestation of resonance properties and quantum conductivity [4,5].

In the present study, we examine the electron–photon interactions in isolated semiconductor QPs (InSb, PbS, HgSe, CdSe) positioned in the interprobe nanogap of a tunneling microscope by measuring and analyzing their current–voltage curves (CVCs). Experiments were performed for random samples of a large number (more than 200) of individual colloidal QPs with TEM (transmission electron microscopy) monitoring of the shape and size of nanocrystals, electron X-ray monitoring of their composition, LB (Langmuir–Blodgett) deposition onto a standard glass substrate with a conductive ITO (indium tin oxide) layer, and CVC measurements under illumination in a tight chamber of a probe microscope. Transmission (Libra-120) and scanning (MiraII LMU) electron microscopes were used to examine the samples. Batches with a minimum QP size spread (with a deviation from mean no greater than $\pm 10\%$) were chosen for study.

CVC measurements performed at room temperature using a SOLVERNano scanning probe microscope and an experimental procedure devised and elaborated in our earlier works [4–6] are central to the present study.

Immediately prior to measurements, nanoparticles were separated from ligands by removing the precipitate through routine centrifugation and redispersion in hexane and deposited in an island monolayer on water subphase with subsequent transfer to a glass substrate with ITO in accordance with the LB process. A proprietary patented setup allowing for monitoring of the process parameters and the fabricated films was used for the purpose [7]. Substrates were made of thin (less than 1 mm) „electronic“ glass with an ITO layer that is produced for LCD screens by Nippon Electric Glass Co., Ltd. The quality of substrates and films deposited on them was verified by TEM and atomic force microscopy. These films were solid monolayers of nanoparticles fixed by cells of the molecular matrix. The distance between nanoparticles varied within the range of 0.1–1 of their size [4].

In order to measure the CVCs of individual QPs, the substrate with a layer was transferred to the object stage of a probe microscope, and the probe was positioned above the chosen nanoparticle. The individual nature of these measurements was guaranteed by the following: QPs had a nonzero gap between them, the probe–sample distance was smaller than the QP size, and the current flow itself was of an electron-by-electron type (one particle

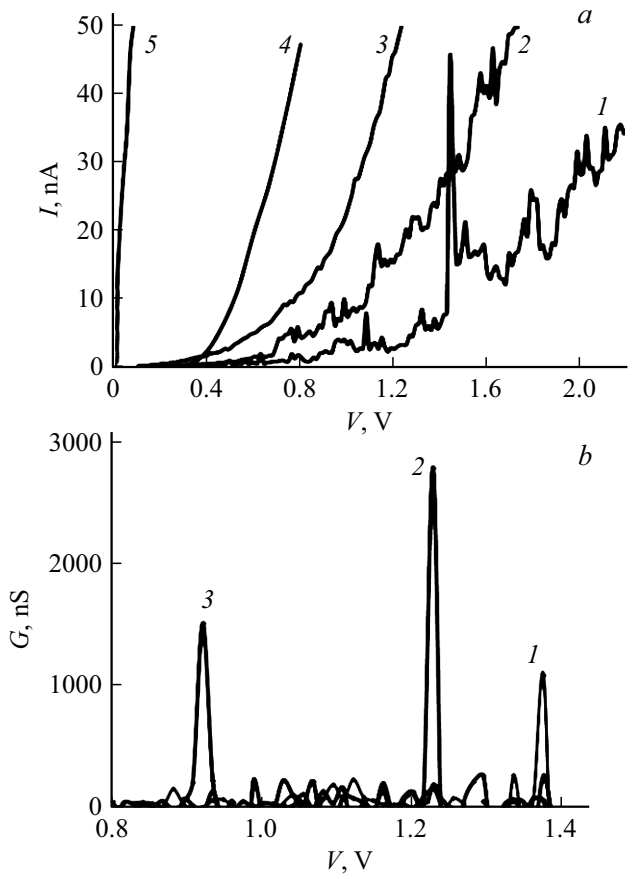

Figure 1. *a* — Typical CVCs: *1–3* — different QPs, *4* — microparticles, *5* — ITO; *b* — quantum conductivity: *1* — QP-PbS, *2* — QP-InSb, *3* — QP-HgSe.

after another), which made simultaneous parallel electron spreading impossible.

Microminiature LEDs with their parameters measured in advance were mounted inside a compact tight light-proof chamber of a tunnel microscope to examine the influence of light on the conductivity of individual QPs. LEDs of a wide spectral range were used: blue — 0.41, green — 0.53, red — 0.64, IR-1 — 0.94, and IR-2 — 1.2 μm. The conditions of single-photon (more exactly, photon-by-photon) irradiation were determined in calculations. Estimates based on the intensity of LED illumination in terms of the photon flux ($\sim 10^{19}\,(\mathrm{sr}\cdot\mathrm{s})^{-1}$), which were obtained under the assumption that each photon produces or excites a non-equilibrium electron in a nanoparticle, demonstrated that their constant number in a QP is below unity, and the current magnitude may be on the order of several nanoamperes. Such values are at the level of reliable measurement in our experiments.

The key results are presented in the table. The semiconductor parameters used in this study (lattice constant a_0 and the ratio of effective electron mass m to free electron mass m_0) were taken from a web-based reference source [8]. The following values are listed in the table: a_n are the nanoparticle sizes measured using TEM images; a_m are the sizes at the maximum of the distribution curve (the primary evaluations and calculations were performed for a_m); and $\tilde{E}_{kn} \sim 0.35k^2(m/m_0)^{-1}a_n^{-2}$ are the dimensional quantization energies obtained by solving the Schrödinger equation (k is the quantum number). Energy is measured in electronvolts, and sizes are given in nanometers [4].

Figure 1, *a* presents the typical CVCs of individual QPs; curves *4* and *5* are for reference (verification).

In our view, different types of CVCs (curves *1–3*) correspond to different degrees of dimensional quantization [4]: curve *1* — strong, *2* — weak, and *3* — zero. In the case of strong quantization, resonance properties are manifested in the form of marked current peaks in CVCs. The strength of these effects is governed by the semiconductor type and the nanoparticle size and may be characterized in the general case by parameter $C \sim (m/m_0)^{-1}a_n^{-2}$ derived from the ratio of a_n and the de Broglie wavelength of an electron [9]. The calculated values of C and the corresponding experimental data on the percentage share (of the total number) of samples with a well-pronounced resonance observed without (p_{dar}) and with (p_{lig}) illumination are listed in the table.

As was demonstrated in our earlier studies (e.g., [4,9]), the behavior of CVCs type *2, 3* (Fig. 1) is governed by the limiting mechanisms of tunneling and charge restriction. In these cases, photoconductivity with a current change factor K depending strongly on the degree of quantization manifests itself in the QP interband absorption spectrum: the lower parameters C and p_{dar} are (Fig. 2 and the table), the higher is K. In addition, quasi-periodic current oscillations (curve *2* in Fig. 1, *a*) may be retained under illumination. In our view, these features may be interpreted physically as manifestations of competition between the processes of carrier photogeneration and dimensional confinement of the electron motion, which gives rise to specific processes: single-electron current and Coulomb restriction. When a QP is illuminated, non-equilibrium electron–hole pairs, which ensure charge neutrality of a QP (thus blocking single-electron restricting effects), are generated. The current through a QP increases greatly as a result, and this is manifested as high-level photoconductivity.

In the model of Coulomb restriction, one needs to take into account the nature of electron transport at the particle–electrode interface, including the influence of surface states subject to the specifics of separation of QPs from organic ligands and their subsequent interaction with atmospheric molecules. As was demonstrated in [4,9], this influence is manifested in the nature of electron tunneling though the interface barrier and, consequently, in the CVC type. A CVC in the scenario without surface states has the $\sim \exp(-AV)$ form, while form $\sim \exp(-B/V)$ corresponds to the scenario involving surface states. Either of these scenarios may arise. However, all electron transport processes manifest themselves in a CVC as limiting ones within a certain voltage interval. This makes it possible to observe them individually in experiments.

Key data

Material	E_g, eV	m/m_0	a_0, nm	a_n, nm	a_m, nm	$\tilde{E}_{kn}$, eV			C	p_{dar}, %	p_{lig}, %	$\Delta\tilde{E}_n$, eV	ΔE, eV
						$\tilde{E}_{k=1}$	$\tilde{E}_{k=2}$	Experiment					
QP-CdSe	1.74	0.13	0.430	2.0–3.5	3.0	0.30	1.20	0.26	1.2	25	41	0.11	0.4–1.3
QP-PbS	0.41	0.080	0.593	2.5–4.0	3.0	0.51	2.05	0.57	1.4	24	28	0.15	0.5–1.4
QP-HgSe	0.07	0.045	0.585	3.5–5.5	4.0	0.49	1.94	0.60	1.5	39	32	0.12	0.4–1.2
QP-InSb	0.17	0.013	0.649	4.5–7.5	5.5	0.89	3.56	0.83	2.5	58	49	0.21	0.8–2.5

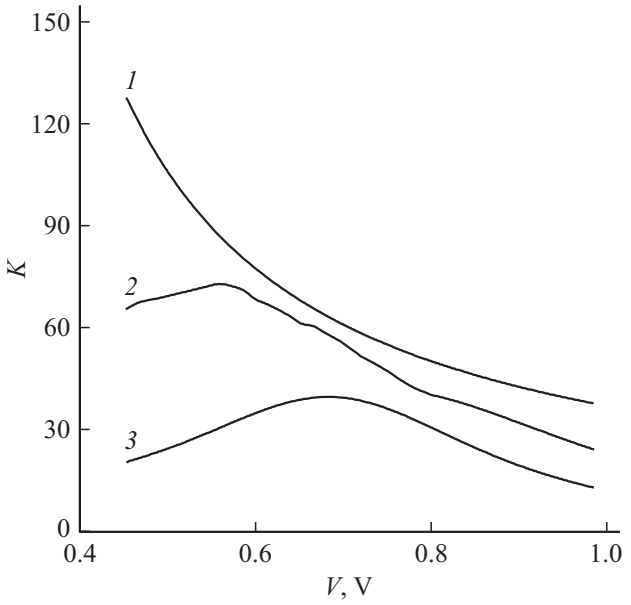

Figure 2. Ratio of the photocurrent to the dark current for samples with CVCs type *2* and *3* in Fig. 1, *a*. *1* — QP-CdSe, *2* – QP-PbS, *3* — QP-InSb.

CVCs type *1* (Fig. 1, *a*) are the result of strong quantum-dimensional confinement of the electron motion in a QP associated with a pronounced resonance of the electron wave process [10]. The resonance peak in a CVC forms or subsides in the process of interaction between an electron and the varying energy of an electric field or a light wave. The inset in Fig. 1, *b* shows the typical dependence of sample conductivity $dI/dV = G$ obtained by differentiating a type *1* CVC (see Fig. 1, *a*). The values of quantum conductivity in the resonance energy region were $\sim (1-3) \cdot 10^{-6}$ S. We estimated them and confirmed the dimensional model of quantum conductivity using the expression for conductivity of a quantum wire per one quantum step with account for the single-electron nature of current [11]: $G_0 \sim kq^2/h$, where q is the electron charge. Assuming that $k = 1$, we find $G_0 \sim 4 \cdot 10^{-5}$ S. Presumably, the $a/a_0 \sim 10$ ratio may be taken as the total number of quantum steps in a nanocrystal. Then, $G \sim G_0/10 \sim 4 \cdot 10^{-6}$ S, which is quite comparable to the experimental results (Fig. 1, *b*).

A thorough analysis of the results of illumination of these samples by LEDs of any one of the used spectral types ($0.4-1.2\,\mu$m) revealed no CVC alterations similar to those found in samples with zero or weak manifestations of dimensional quantization and resonance. This is attributable to the fact that a non-equilibrium electron in the resonance state injected into a QP blocks interband transitions of valence electrons (interband Coulomb blockade) and intraband interlevel transitions. From the physical standpoint, this blockade is effected due to the fact that the probability of finding an electron at any site within a nanoparticle under confinement is near-unity. Therefore, only one non-equilibrium quasi-free (conduction) electron may be present in a particle, blocking any other electrons (including those of interband and intraband interlevel transitions) by its field.

A non-equilibrium quasi-free electron may be heated under these conditions in a QP (as in a quantum well) by the electric field of a light wave [12]. The field intensity in this scenario (a lower-bound estimate of which is 10^4-10^5 V/cm in the present case) is 1–2 orders of magnitude higher than the minimum threshold value for the heating effect calculated in [12].

Figure 3 shows the CVC variations driven by such processes under illumination. Two types of variations are observed: (1) shift of resonance peaks toward lower voltages (curves *1* and *1′*); (2) vanishing of a peak (curves *2* and *2′*). In our view, the light energy is imparted to an electron in the former case via heating by the electric field, which induces a resonance at lower voltages. In the latter case, an electron should undergo a transition from a lower quantum state with a relatively low energy to an upper state with a higher energy. Apparently, the added energy of a light wave is not sufficient to induce this transition. The variation of percentage p_{lig} of samples, which increases under illumination at lower values of parameter C and decreases at higher C (see the table), may be explained in roughly the same way.

Given that a non-equilibrium electron injected into a QP is not free, it is fair to make an assumption that the heating of a quasi-bound electron by the field of an electromagnetic wave is, in contrast to the mechanism of intersubband absorption and transitions [13], „step-type." In our view, the essence of this heating model is that an electron subjected to illumination undergoes a transition from one stable resonance state to another in certain energy

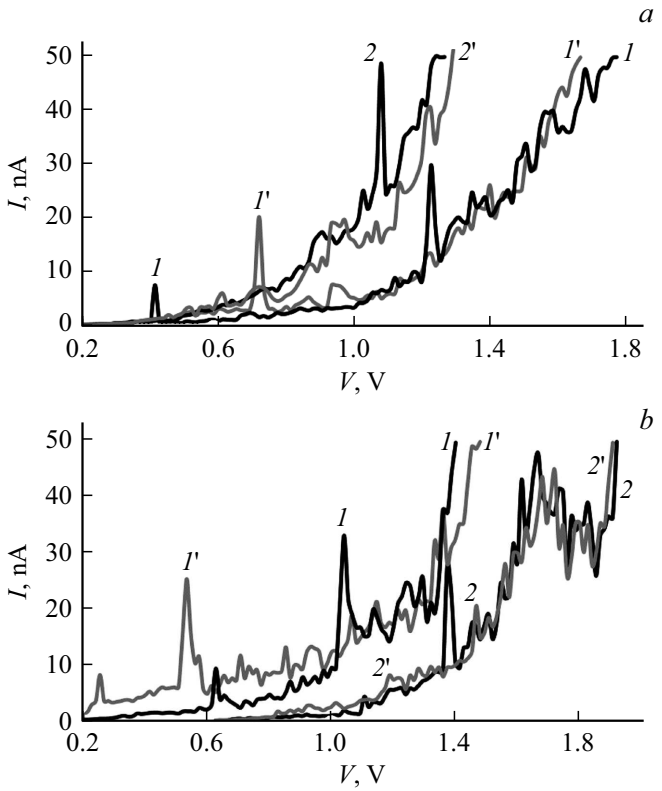

Figure 3. CVCs for intraband transitions. *a* — PbS, *b* — InSb. *1*, *2* — Dark CVC, *1′*, *2′* — light CVC (IR-2). *1*, *1′* — Shift of resonance peaks toward lower voltages, *2*, *2′* — vanishing of a peak.

steps specified by the lattice constant (similar to Bloch oscillations [14]). Energy step $\Delta\tilde{E}_n$ may be written as differential

$$\Delta\tilde{E}_n \sim (d\tilde{E}_{kn}/da_n)a_0 \sim 0.7k^2(a_n)^{-3}(m/m_0)^{-1}a_0,$$

while the transition energy for resonance $k = 1$ is given by

$$\Delta V \sim \Delta E \sim \Delta\tilde{E}_n(a_n/a_0) \sim 0.7(a_n)^{-2}(m/m_0)^{-1}.$$

The calculated values of $\Delta\tilde{E}_n$ and ΔE are listed in the table and roughly correspond to experimental data. The minimum values of energy step $\Delta\tilde{E}_n$ are at the level of 100 meV.

Thus, photoconductivity for interband carrier transitions, which is induced by lifting of the blockade by single-electron current and the Coulomb restriction, is observed in quantum-dimensional particles of InSb, PbS, HgSe, and CdSe semiconductors. In the context of dimensional quantization, the observed resonance current peaks vanish or shift toward lower energies under illumination. This is attributable to heating of a non-equilibrium electron by the electric field of a light wave. The energy minimum of influencing and detected radiation quanta may be estimated at 100 meV. The obtained results may find application in the design of uncooled IR detectors (single-photon ones included).

Funding

This study was supported by grant 20-07-00603 from the Russian Foundation for Basic Research.

Conflict of interest

The authors declare that they have no conflict of interest.

References

[1] A.I. Arzhanov, A.O. Savostyanov, K.A. Magaryan, K.R. Karimullin, A.V. Naumov, Photonics Russ., **15** (8), 622 (2021). DOI: 10.22184/1993-7296.FRos.2021.15.8.622.641
[2] A. Gorodetsky, I.T. Leite, E.U. Rafailov, Appl. Phys. Lett., **119**, 111102 (2021). DOI: 10.1063/5.00627201
[3] N.R. Abdullah, C.-Sh. Tang, A. Manolescu, V. Gudmundsson, Physica B, **641**, 414097 (2022). DOI: 10.1016/j.physe.2020.113996
[4] N.D. Zhukov, M.V. Gavrikov, Tech. Phys. Lett., **48** (4), 56 (2022). DOI: 10.21883/TPL.2022.04.53174.19090.
[5] S.A. Sergeev, M.V. Gavrikov, N.D. Zhukov, Tech. Phys. Lett., **48** (5), 26 (2022). DOI: 10.21883/TPL.2022.05.53472.19115.
[6] N.D. Zhukov, M.V. Gavrikov, Mezhdunar. Nauchno-issled. Zh., No. 8-1 (110), 19 (2021) (in Russian). DOI: 10.23670/IRJ.2021.110.8.004
[7] I.A. Gorbachev, S.N. Shtykov, G. Brezesinski, E.G. Glukhovskoy, BioNanoScience, **7**, 686 (2017). DOI: 10.1007/s12668-017-0404-4
[8] http://xumuk.ru/encyklopedia
[9] N.D. Zhukov, M.V. Gavrikov, S.N. Shtykov, Semiconductors, **56** (4), 269 (2022). DOI: 10.21883/FTP.2022.06.52588.9809
[10] G.F. Glinskii, Tech. Phys. Lett., **44** (3), 232 (2018). DOI: 10.1134/S1063785018030161].
[11] N.T. Bagraev, A.D. Buravlev, L.E. Klyachkin, A.M. Malyarenko, W. Gehlhoff, V.K. Ivanov, I.A. Shelykh, Semiconductors, **36** (4), 439 (2002). DOI: 10.1134/1.1469195.
[12] L.E. Vorob'ev, S.N. Danilov, V.L. Zerova, D.A. Firsov, Semiconductors, **37** (5), 586 (2003). DOI: 10.1134/1.1575366.
[13] L.E. Vorob'ev, V.Yu. Panevin, N.K. Fedosov, D.A. Firsov, V.A. Shalygin, S. Hanna, A. Seilmeier, Kh. Moumanis, F. Julien, A.E. Zhukov, V.M. Ustinov, Phys. Solid State, **46** (1), 118 (2004). DOI: 10.1134/1.1641936.
[14] I.A. Dmitriev, R.A. Suris, Semiconductors, **35** (2), 212 (2001). DOI: 10.1134/1.1349935.